



# Experimental analysis of phase change phenomenon of paraffin waxes embedded in copper foams



Simone Mancin <sup>a,\*</sup>, Andrea Diani <sup>b</sup>, Luca Doretto <sup>c</sup>, Kamel Hooman <sup>d</sup>, Luisa Rossetto <sup>b</sup>

<sup>a</sup> Università degli Studi di Padova, Dipartimento di Tecnica e Gestione dei Sistemi Industriali, Stradella S. Nicola, 3, 36100 Vicenza, Italy

<sup>b</sup> Università degli Studi di Padova, Dipartimento di Ingegneria Industriale, Via Venezia 1, 35131 Padova, Italy

<sup>c</sup> Università degli Studi di Padova, Dipartimento di Ingegneria Civile, Edile e Ambientale, Via Marzolo 9, 35131 Padova, Italy

<sup>d</sup> The University of Queensland, School of Mechanical and Mining Engineering, Brisbane St Lucia, QLD 4072, Australia

## ARTICLE INFO

### Article history:

Received 15 April 2014

Received in revised form

15 October 2014

Accepted 12 November 2014

Available online 6 January 2015

### Keywords:

Phase change materials

PCM

Foam

Paraffin

Electronic cooling

## ABSTRACT

This paper presents an experimental investigation of the solid–liquid phase change process of three natural paraffin waxes, which show slightly different melting temperature: 53 °C, 57 °C, and 59 °C, at three heat fluxes: 6.25, 12.5, and 18.75 kW m<sup>-2</sup>. Furthermore, the use of copper foams to improve the phase change process is experimentally studied by employing three different samples with 5, 10, and 40 PPI and constant porosity equal to 0.95. The experimental results clearly show that the presence of the foam matrix improves the heat transfer capabilities of the passive system allowing for lower surface temperature compared to no-foam case, at the same imposed heat flux. A direct video visualization of the process also permitted to show the effects of the porous medium on melting and solidification processes.

© 2014 Elsevier Masson SAS. All rights reserved.

## 1. Introduction

It is well known that the heat transfer associated with a phase change process is much higher than sensible enthalpy change even in forced convection. In particular, the vaporization process has been widely studied because it exploits the highest heat transfer coefficient; this heat transfer mechanism is used in both passive (i.e. heat pipes) and active (i.e. refrigerating machines) cooling devices. However, the solid–liquid phase change process is another interesting possibility to reject even high heat loads, especially when they are intermittent. The term Phase Change Materials (PCMs) commonly refers to those materials, which use the solid–liquid phase change process to adsorb and then release heat loads. In the last decade, the use of PCMs as heat storage in passive heat transfer device has been widely studied both analytically and experimentally. The use of the latent heat absorption phenomenon associated with melting of a suitable PCM can be considered an

effective way to delay or modify the temperature rise of a surface subjected to high and intermittent heat fluxes. The intrinsic advantage of the PCM systems is related to their simplicity and reliability; however, the reversible phase change process must be carefully analysed in order to avoid any unmanageable situations during the real operation of these devices.

As described in several comprehensive reviews [1–3] published in the open literature, PCMs have been widely proposed for thermal storage applications due to their capability of storing and releasing large amounts of energy with a small PCM volume and a relatively low temperature variation.

As described by Sharma et al. [2], a large number of phase change materials (organic, inorganic, and eutectic) are available in any required temperature range. An ideal PCM should exhibit a suitable phase-transition temperature, high latent heat of fusion, and high thermal conductivity; it should be characterized by high density associated with a small volume change during the melting process and low vapour pressure in the melt; moreover, it should be chemically stable over a long period of time, non-toxic and non-hazardous, and compatible with the constructional materials. Finally, it should be abundant, available, and cost effective.

Amongst the available PCMs, paraffin waxes have been found to exhibit many desirable characteristics, such as high latent heat, low

\* Corresponding author. Tel.: +39 0444 998746.

E-mail addresses: [simone.mancin@unipd.it](mailto:simone.mancin@unipd.it) (S. Mancin), [andrea.diani@unipd.it](mailto:andrea.diani@unipd.it) (A. Diani), [luca.doretto@unipd.it](mailto:luca.doretto@unipd.it) (L. Doretto), [k.hooman@uq.edu.au](mailto:k.hooman@uq.edu.au) (K. Hooman), [luisa.rossetto@unipd.it](mailto:luisa.rossetto@unipd.it) (L. Rossetto).

### Nomenclature

$a_{sv}$	surface area per unit of volume [ $\text{m}^{-1}$ ]
$c_p$	specific heat at constant pressure [ $\text{J kg}^{-1} \text{K}^{-1}$ ]
HF	heat flux [ $\text{kW m}^{-2}$ ]
$l$	fibre length [m]
PCM	Phase Change Material [–]
PPI	Pores Per Inch [ $\text{in}^{-1}$ ]
$t$	fibre thickness [m]
$T_{\text{melt}}$	melting temperature [ $^{\circ}\text{C}$ ]

### Greek symbols

$\varepsilon$	porosity [–]
$\lambda$	thermal conductivity [ $\text{W m}^{-1} \text{K}^{-1}$ ]
$\rho$	density [ $\text{kg m}^{-3}$ ]
$\rho_p$	relative density [–]

vapour pressure in the melt, chemically inert and stable, non-toxic. However, they also have a very low thermal conductivity and a high volume change during the melting process. In some cases, the paraffin waxes can also be flammable. Thus, heat transfer enhancement techniques are required for their possible implementation in PCM passive cooling devices and thermal storage applications [4]. As such, several researchers have focused their attention to different enhancement techniques proposed to improve the thermal conductivity of the PCMs; Jegadheeswaran and Pohekar [5] and Fan and Khodadadi [6] have reviewed most of these efforts.

Baby and Balaji [7] experimentally investigated different enhancement techniques to improve the performance of PCM heat sinks for electronic equipment cooling; in particular, the authors explored the use of heat sinks with pin fin and plate fin geometries with phase change materials for thermal management of portable electronic devices. The effect of different types of fins at different power levels in enhancing the operating time for different set point temperatures and on the duration of latent heating phase were explored. An enhancement factor of 18 was obtained in the operation time for a pin fin heat sink as compared to that of the heat sink without fins.

The same authors [8] conducted an experimental optimization of different PCM based pin fin aluminium heat sinks; paraffin wax and n-eicosane were used as PCMs. Using n-eicosane embedded in a 72 pin fins heat sink, the authors found a 24-fold heat transfer enhancement compared with no-fin case. According to those authors, a large number of uniformly distributed fins are largely responsible for this enhancement in heat transfer.

In a subsequent study, Baby and Balaji [9] have experimentally investigated the effect of heat transfer performance of a PCM based plate fin heat sink matrix under constant and intermittent heat loads. Furthermore, the necessity to quantitatively characterize the behaviour of such heat sinks under intermittent operation was highlighted as a design based on continuous heat duty might lead to oversized, more expensive and sub-optimal heat sinks.

Fan et al. [10] investigated the effects of melting temperature and the presence of internal fins on the performance of a PCM based heat sink for thermal management of electronics. The comparisons were made between two PCMs with similar thermo-physical properties but different melting temperatures at various intensive pulsed heat loads. N-eicosane with a nominal melting temperature of  $37^{\circ}\text{C}$  and 1-hexadecanol with a nominal melting temperature of  $49^{\circ}\text{C}$  were studied. According to those authors, the use of a PCM with a rationally high melting temperature, limited by the temperature of the cooling target, could extend a longer time of

protection from overheating. The use of internal fins can improve the performance of the PCM-based heat sink. In the studied cases, the maximum temperature rise was lowered by up to  $10^{\circ}\text{C}$  for the finned heat sink.

Mahmoud et al. [11] studied the effects of PCM material, heat sink designs and power levels on PCM based heat sinks performance for cooling electronic devices. Six PCMs were used including paraffin wax, two materials based on mixture of inorganic hydrated salts, two materials based on mixture of organic substances and one material based on a mixture of both organic and inorganic material. Results showed that increasing the number of fins can enhance heat distribution to PCM leading to lower heat sinks peak temperatures. Furthermore, it was reported that the material with the lowest melting temperature showed the best performance in terms of lowest operating temperature and longest duration of low heat sink temperatures.

Kozak et al. [12] experimentally and numerically investigated a hybrid PCM-air heat sink using eicosane as PCM. The experiments were conducted at room and elevated ambient temperatures. A simplified numerical model was developed and successfully compared with the experimental results.

Heat transfer enhancement of PCM-based heat sinks can also be obtained using porous matrix as the thermal conductivity enhancer instead of fins. Many studies considered the enhancement of heat transfer through PCM using porous media. Among these works, Hong and Herling [13] experimentally analysed the effects of geometric parameters of open-cell aluminium foams on the performance of aluminium foam-PCM heat sinks. The authors used a paraffin wax as PCM. For the aluminium foam specimens filled with the PCM, both the heating and cooling times were significantly larger than those with the aluminium foam specimens without the PCM.

The use of carbon foam matrices saturated with paraffin wax for thermal protection purposes was studied by Mesalhy et al. [14]. The effects of the porosity and thermal properties of a porous medium filled with PCM were studied numerically and experimentally. The results showed that the porosity and thermal conductivity of the matrix play important roles in the thermal performance of the system.

Zhao et al. [15] used paraffin wax RT58 as PCM, in which metal foams are embedded to enhance the heat transfer. The test samples were electrically heated on the bottom surface with a constant heat flux. The authors found that the addition of metal foam can increase the overall heat transfer rate by 3–10 times (depending on the metal foam structures and materials) during the melting process and the pure liquid zone.

Tian and Zhao [16] performed numerical investigations of heat transfer in PCMs kept in porous metals. Significantly higher conduction heat transfer rates were reported with the use of metal foams as a consequence of their higher thermal conductivities. On the other hand, higher flow resistance posed by foams suppresses natural convection. All in all, it was noted that enhancement of heat conduction offsets the natural convection loss and, overall, a better heat transfer performance was achieved.

Zhou and Zhao [17] experimentally investigated the heat transfer characteristics of two different PCMs (RT 27 paraffin wax and calcium chloride hexahydrate) embedded in open-cell metal foams and expanded graphite. The results indicated that the use of porous materials, either open-cell metal foams or expanded graphite, can enhance the heat transfer rate of PCMs. Furthermore, metal foams can provide better heat transfer performance than expanded graphite due to their continuous interconnected structures.

Cui [18] compared the charging performance of paraffin wax with and without copper foam. The results indicated that the foam

material not only led to a more uniform temperature distribution within the thermal energy storage unit, but also extensively reduced the charging time.

Baby and Balaji [19] experimentally studied the enhancement and the effect of orientation of a copper porous matrix filled with n-eicosane as PCM. The copper foam was found to enhance the thermal performance of the PCM heat sink while the orientation does not have any significant impact on its performance.

More recently, Thapa et al. [20] experimentally studied the effect of a copper foam and a copper matrix on the phase change process of a paraffin wax. The authors found that in both cases the heat transfer performance improved compared with the bare paraffin. Furthermore, the authors found that the copper matrix performed similarly to the foam. It is interesting to point out that neither the copper matrix nor the copper foam were physically attached to the heater; thus, a non-negligible thermal resistance might be present. The authors also ran a numerical study to estimate the effect of the apparent thermal conductivity on the heat transfer. The results indicated diminishing returns as conductivity exceeded  $4\text{--}6\text{ W m}^{-1}\text{ K}^{-1}$ .

From this overview, one notes the great interest of the scientific community in solutions that can enhance the heat transfer performance of PCM based heat sinks. As an outcome, the use of metal foams represents a viable solution to achieve these results especially when paraffin waxes are used as PCMs. On the other hand, none of the cited works conducted a systematic and comprehensive analysis of the use of metal foams: Zhoua and Zhao [17], Cui [18], Baby and Balaji [19], and Thapa et al. [20] analysed one foam sample which does not allow the analysis of the foam properties. Hong and Herling [13] varied the pore density (from around 10 to 50 PPI), while Zhao et al. [15] compared the results obtained with a 10 PPI 95% porosity foam with two other samples with 30 PPI and porosity of 85% and 95%. Moreover, apart from Zhao et al. [15] and Zhoua and Zhao [17] who tested foams sintered on metal substrates, a proper contact between the metal foam and the heated wall was not ensured in the other papers. Note that the benefits obtained using the metal foams as heat transfer medium would be completely lost or undermined if the foam-surface thermal contact is not minimized to a certain level. For instance, a low thermal conductivity contact layer, comprised of paraffin, can significantly reduce the overall heat transfer rate; see Refs. [21–23]. Finally, it also appears that the size of the samples varied from one work to another leading to different imposed heat fluxes and boundary conditions in the works reported in the open literature.

As highlighted, among the different PCMs studied in the open literature, the paraffin waxes seem to exhibit many desirable

characteristics but they also have two main drawbacks: a low thermal conductivity and a high volume change during the melting process. The possible solution of these two issues can improve the applicability of these PCMs to the heat transfer systems. From this standpoint, there is a lack of works that systematically analyse the performance of the paraffin waxes as PCMs and how it would be possible to mitigate and/or eliminate their applicability issues. This work aims at investigating the use of the paraffin waxes as PCMs, with and without metal foams, in order to understand the effects of both the type of paraffin and the metal foam characteristics on the phase change process at different imposed heat fluxes.

In particular, this paper experimentally studies the phase change performance of three different paraffin waxes with similar melting temperatures at three different heat fluxes:  $6.25$ ,  $12.5$ , and  $18.75\text{ kW m}^{-2}$ . Furthermore, three different off-the-shelf copper foams with 5, 10, and 40 PPI are used as heat transfer medium to build paraffin-foam systems to enhance the phase change process and compensate for low thermal conductivity of the PCM leading to a lower and more uniform temperature distribution in the heat sink.

## 2. Experimental setup

The experimental setup consists of three main components: the test module, the power supplier, and the data acquisition system. As shown in Fig. 1a, the test module was designed to permit the direct visualization of the phase change process. A 10 mm thick copper plate of size  $40 \times 40\text{ mm}^2$  was used as the spreader, three 10 mm thick Bakelite walls, and a 10 mm thick piece of glass were used to confine the paraffin wax during the test. The walls and the base were jointed using a high temperature two-component epoxy resin. Five holes were drilled on one of the Bakelite side-walls to insert as many T-type thermocouples inserted in 1 mm thick stainless steel probes, four of those were fixed 20 mm inside the module along the centreline every 10 mm starting from 5 mm over the heated base. The fifth T-type thermocouple probe was inserted in a hole drilled just over the centre of the copper spreader in order to monitor the junction temperature. The Bakelite–glass module was then inserted in a Teflon housing (Fig. 1b) designed to ensure similar boundary conditions in all of the tests permitting a direct comparison between the different paraffin waxes and also amongst the foam-paraffin solutions. Furthermore, an additional layer of 20 mm thick insulating material was added to minimize heat losses from the test section. The Bakelite-glass module was located above the heater, which consists of another  $40 \times 40\text{ mm}^2$  copper plate where a guide was milled to insert a Ni–Cr wire resistance. The heater was located in a groove milled into the base of the teflon

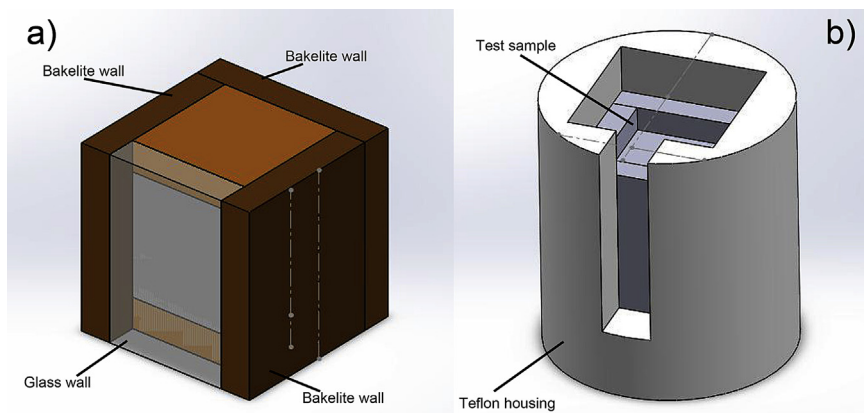


Fig. 1. Bakelite–glass module (a) and test module assembly (b).

housing. A highly conductive silicon-based paste was used to reduce the thermal contact resistance between the copper spreader of the bakelite–glass module and the heater and to ensure a uniform distribution of the heat all over the heated base.

The videos were recorded using the frontal glass window shown in Fig. 1, which was sealed with additional insulating material during the tests when video recording was not on.

Five additional calibrated T-type thermocouples were used to monitor the Teflon external wall temperature. In all investigated cases, the same boundary conditions were found, thus the results relative to different paraffin waxes and foam-paraffin systems can be considered comparable.

In the case of foam–paraffin module, the Bakelite and glass walls were attached directly to the bottom copper plate of the foam samples. The copper foams were obtained from the bigger samples previously tested during air forced convection experiments by Mancin et al. [24]. The  $40 \times 40 \times 40 \text{ mm}^3$  copper samples used in this work were obtained by cutting the  $100 \times 100 \times 40 \text{ mm}^3$  samples using the electro-erosion machining technique. This cutting technique was selected because it preserves the foam structure during the machining process.

An example of the obtained samples is shown in Fig. 2, where a photo of a 10 PPI copper foam is shown. The top plate was then cut in order to deposit the liquid paraffin wax into the module.

The T-type thermocouple stainless steel probes were connected to a Kaye 170 ice-point reference and then recorded using HP 34970A multimeter. The whole chains were calibrated using a thermostatic bath and a high accuracy (i.e.  $\pm 0.02 \text{ K}$ ) Pt100. The resulting individual calibration curves allow for an uncertainty of  $\pm 0.1 \text{ K}$  in the temperature measurements. The other T-type thermocouples were also calibrated and present an uncertainty of  $\pm 0.05 \text{ K}$ .

The electrical power supplied to the module is indirectly measured by means of a calibrated reference resistance (shunt) and by the measurement of the effective EDP (Electrical Difference Potential) of the resistance wire inserted in the copper heater. The current is calculated from Ohm's law. The error propagation analysis applied to this measurement leads to an estimated uncertainty of  $\pm 0.13\%$  of the reading.



Fig. 2. Photo of a 10 PPI copper foam sample.

Table 1

Most important thermophysical properties of the tested paraffin waxes.

Type	$T_{\text{melt}} [^{\circ}\text{C}]$	$c_p [\text{J kg}^{-1} \text{K}^{-1}]$	$\lambda [\text{W m}^{-1} \text{K}^{-1}]$	$\rho [\text{kg m}^{-3}]$
SASOLWAX 5203	52–54			
SASOLWAX 5603	56–58	1800 at 20 °C	0.25	920 at 20 °C
SASOLWAX 5803	58–60	2400 at 70 °C		777 at 70 °C

### 3. Paraffin waxes and foam matrixes

Three different paraffin waxes were selected: SASOLWAX 5203, SASOLWAX 5603, SASOLWAX 5803. These PCMs are only distinguished by their different melting temperatures being 53 °C, 57 °C, and 59 °C, respectively. The thermal conductivity of these materials is around  $0.25 \text{ W m}^{-1} \text{K}^{-1}$ , the solid density at 20 °C is  $990 \text{ kg m}^{-3}$  while that of the liquid is  $770 \text{ kg m}^{-3}$ , the specific heat at constant pressure at 20 °C is  $1800 \text{ J kg}^{-1} \text{K}^{-1}$  whereas at 70 °C it becomes  $2400 \text{ J kg}^{-1} \text{K}^{-1}$ . The selected paraffin waxes were not flammable. Their thermophysical properties are listed in Table 1.

Considering the investigated porous structures, three different copper foam samples were machined from bigger ones with 5, 10, and 40 PPI and a constant porosity of around 0.94. Mancin et al. [24] measured the fibre thickness and length of the samples and, according to the data listed in Table 2, those values decrease as the number of pores per inch increase. Another important parameter of the foam structure reported in Table 2 is the surface area per unit volume  $a_{sv}$ , which increases from  $292 \text{ m}^{-2}$  of the 5 PPI sample to  $1611 \text{ m}^{-2}$  of the 40 PPI one. The foam structures are brazed to the copper bases, thus the thermal contact resistance between the two materials can be neglected.

### 4. Modules preparation

As described before, two different kinds of modules were prepared: no-foam PCM module and foam-paraffin ones. With the former, the empty Bakelite-glass module was filled up with the paraffin wax covering the top thermocouple, which defined the level. The paraffin waxes show a volume change associated with the phase change process of about 10–15%. Commensurate with that, during solidification, which occurred from the sides to the centre, a deep hole was generated by the volume contraction. The central holes were continuously filled up using additional paraffin wax till no contraction was observed.

The high volume change value represents the main drawback of the paraffin waxes when considered as possible PCMs for heat transfer applications. The main related consequence of this characteristic is linked to real operation of the PCM device under thermal cycles: the void that is generated at the centre of the system during the solidification process may imply an unmanageable behaviour during the succeeding cycle.

Table 2

Major characteristics of the foam structures.

	Cu-5–6.5	Cu-10–6.6	Cu-40–6.4
Number of pores per inch, PPI <sup>a</sup> [ $\text{in}^{-1}$ ]	5	10	40
Relative density, $\rho_R^a$ [%]	6.5	6.6	6.4
Porosity, $\epsilon$ [–]	0.935	0.934	0.936
Fibre thickness, $t^b$ [mm]	0.495	0.432	0.244
Fibre length $l^b$ [mm]	1.890	1.739	0.999
Surface area per unit of volume, $a_{sv}$ [ $\text{m}^2 \text{m}^{-3}$ ]	292	692	1611

<sup>a</sup> Measured by the manufacture ERG Aerospace – [www.ergaerospace.com](http://www.ergaerospace.com).

<sup>b</sup> Measured by Mancin et al. [24].

The foam-paraffin module is obtained by filling up the foam matrix with liquid paraffin wax. In this case, the matrix is cooled down uniformly and thus the composite foam-paraffin solid did not present any void volume.

This represents a preliminary important achievement, the use of the foam as matrix for a PCM device mitigates one of the main drawbacks of the paraffin waxes as phase change materials for thermal management.

## 5. Experimental results

Preliminary tests were conducted to analyse the different heat transfer performance of the three paraffin waxes without the foam matrix. Three heat fluxes were imposed: 6.25, 12.5, and 18.75 kW m<sup>-2</sup>, corresponding to 10, 20, and 30 W, respectively, over a 40 × 40 mm<sup>2</sup> surface area. The selected heat loads refer to those encountered in the lighting industry in particular light-emitting diodes (LEDs); see for instance [<http://www.cree.com/>]. Besides, the maximum value was kept at 30 W in order to avoid any safety issues related to the high wall temperature, which as it will be shown later, can exceed 120 °C in the case of no-foam PCM module.

Fig. 3 reports the temperature profiles recorded during the melting process of the paraffin 5203 at HF = 6.25 kW m<sup>-2</sup>; as described before, five calibrated T-type thermocouples were located along the centreline of the module. The junction temperature is measured inside the copper spreader, whereas the other four probes are positioned inside the paraffin at 5, 15, 25, and 35 mm from the heated base. The junction temperature monotonically increases, whereas the temperature gradient decreases as the heat transfer process proceeds. In particular, the phase change process can be subdivided in two parts: the first one ends after 1500–1600 s (i.e. 25–26 min) and it is characterized by a sharp increase in junction temperature and by the  $H = 5$  mm thermocouple readings. In fact, the junction temperature reaches around 68 °C in the first 1500 s, while the maximum temperature after around 6000 s is just above 80 °C.

In the first part of the test, the heat is transferred through the paraffin by conduction, this is confirmed by the temperature profile measured at  $H = 5$  mm where a linear increase in temperature is noted. When the liquid paraffin reaches the thermocouple, the temperature suddenly increases and quickly approaches the asymptotic value of 67–68 °C, around 15 °C above that of melting ( $T_{\text{melt}} = 53$  °C).

It is worth to underline that the liquid paraffin becomes superheated before the whole phase change process is completed

because the low thermal conductivity of the paraffin inhibits the heat transfer through the solid part. This may result in a greater junction temperature; the possible enhancement of the thermal conductivity of the solid part might improve the phase change process keeping the junction temperature at lower values.

The other three thermocouples show similar exponential temperature profiles, their temperature gradients increase as the liquid front moves towards their positions. At the end of the fusion, the temperature of the liquid paraffin remains almost 15 °C higher than that of melting ( $T_{\text{melt}} = 53$  °C). Tests deemed completed as soon as the melting front reached the top ( $H = 35$  mm) thermocouple.

Similar temperature profiles were recorded at all investigated heat fluxes and for all the studied paraffin waxes. For the sake of brevity, the other test results are not reported and some interesting comparisons are proposed in what follows.

Fig. 4 compares the temperature profiles recorded by the junction thermocouple during the phase change process of paraffin 5203 at three different heat fluxes: 6.25, 12.5, and 18.75 kW m<sup>-2</sup>. These tests highlight the performance of the paraffin wax as a function of the heat flux, allowing for the understanding of its limitation in terms of maximum temperature and cooling time for a given power input.

As expected, the final temperature increases as the heat flux increases reaching around 80 °C, 100 °C, and 120 °C at 6.25, 12.5, and 18.75 kW m<sup>-2</sup>, respectively. The test ends earlier as the heat flux increases. In fact, it ends after 2100 s (i.e. 35') at HF = 18.75 kW m<sup>-2</sup>, after 2800 s (i.e. 47') at HF = 12.5 kW m<sup>-2</sup>, and after 6500 s (i.e. 1 h 48') at HF = 6.25 kW m<sup>-2</sup>.

The three studied paraffin waxes are compared in Fig. 5, where the junction to ambient temperature difference profiles are plotted against time at HF = 6.25 kW m<sup>-2</sup>. From a general standpoint, there is not any noticeable difference between the curves. The paraffin wax 5603 ( $T_{\text{melt}} = 57$  °C) shows the lowest temperatures, while the 5803 ( $T_{\text{melt}} = 59$  °C) exhibits the highest values; the 5203 presents an intermediate behaviour. At higher heat flux, the behaviour of the three paraffin waxes was almost the same but no one showed the lowest temperatures at all the imposed heat fluxes. For this reason, it was decided to use paraffin 5203 in the tests with the metal foams.

The temperature profiles plotted in Fig. 6 as a function of the time exhibit a different behaviour during the phase change process of the 5203 paraffin wax at HF = 6.25 kW m<sup>-2</sup>. In this case, the PCM was poured into a 5 PPI copper foam with a porosity of 94%. As seen, all the thermocouples readings are more or less the same. Considering the junction temperature, it monotonically increases and, at the end of the test, the junction temperature reaches around

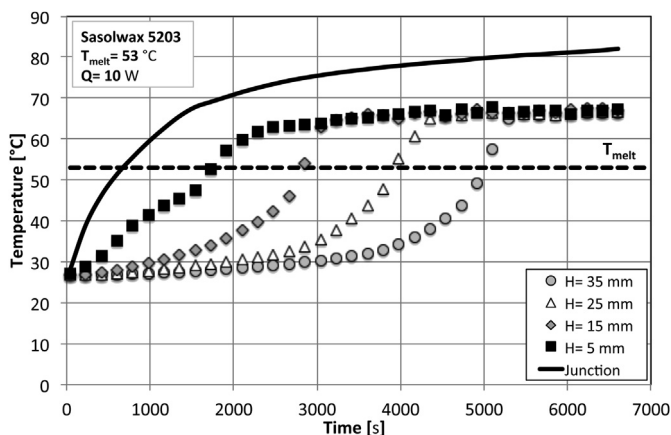


Fig. 3. Temperature profiles recorded during the phase change process at HF = 6.25 kW m<sup>-2</sup> for the paraffin 5203 without foam matrix.

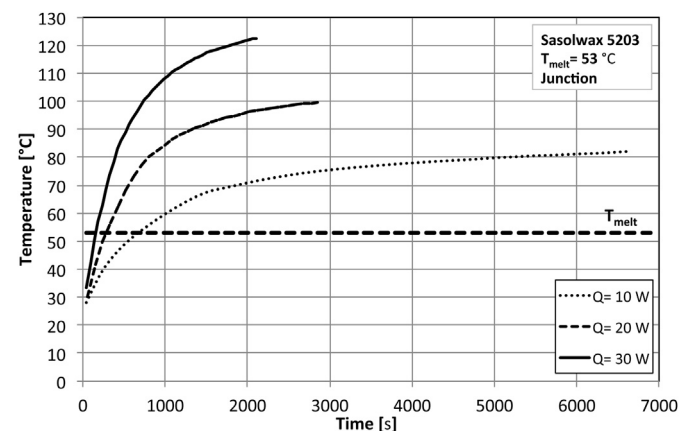


Fig. 4. Effects of the imposed heat flow rate on the phase change process of the paraffin wax 5203.

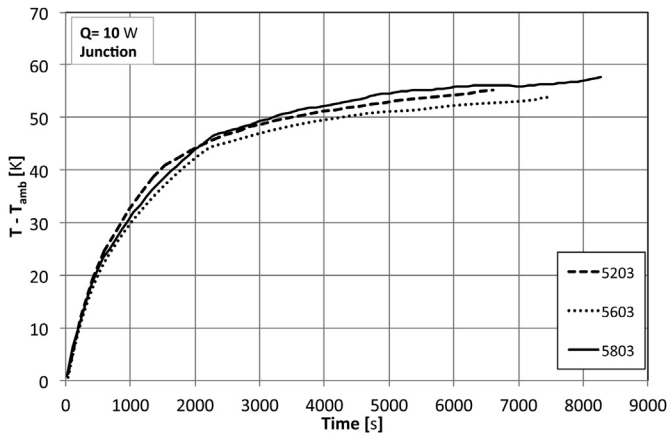


Fig. 5. Comparison between the three paraffin waxes at constant imposed heat flow rate of 10 W.

70 °C (at 6000 s), which is almost 10 °C lower than that measured without the foam.

From the plotted temperature profiles, one notes that the foam allows for a uniform distribution of the heat. The heat is transferred through the foam structure as confirmed by the temperature difference between the junction and the top thermocouples which is always limited to 6–8 °C. Similar results were also found by Zhao et al. [15], who highlighted that the temperature difference across the PCM embedded in the foam was never higher than 10 °C.

According to the temperature profiles plotted in Fig. 3, the maximum temperature difference recorded during the phase change process of 5203 paraffin wax without the foam was around 45 °C.

When comparing the temperature profiles plotted in Figs. 3 and 6, it can be noticed that, without the copper foam structure, the junction temperature reaches the value of 70 °C after 2000 s whereas in the case with foam, this value is reached after 6000 s. Furthermore, even if the phase change process starts later when the paraffin is embedded in the foam as compared to the case without foam, it finishes earlier as it can be seen following the temperature profile of the top thermocouple ( $H = 35$  mm). Here, with foam, it reaches the melting temperature after around 4000 s while without foam this time is 5000 s.

This is confirmed by the results measured at  $HF = 12.5 \text{ kW m}^{-2}$  (i.e. 20 W) as reported in Fig. 7 where the cases with and without

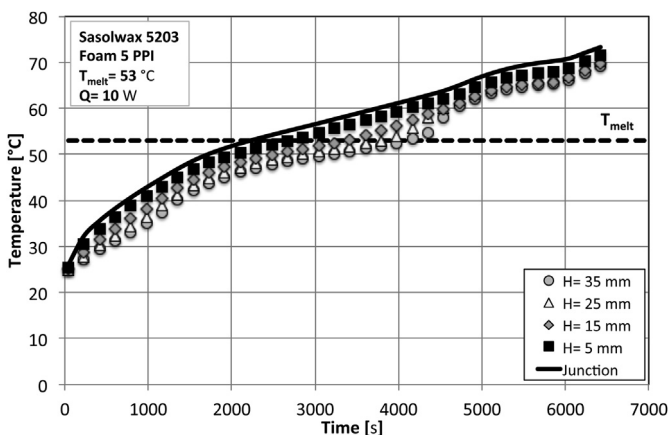


Fig. 6. Temperature profiles of 5 PPI copper foam embedded with paraffin wax 5203 at  $Q = 10$  W.

5 PPI foam are compared. The images reported in Fig. 7 are taken from the video 1, which is also available in the supplementary data. Starting from the top diagram, the dotted lines refer to the case without foam while the continuous solid lines to the case with the 5 PPI foam.

Supplementary video related to this article can be found at <http://dx.doi.org/10.1016/j.ijthermalsci.2014.11.023>.

- No evidence of fusion is observed during the first 10 min (i.e. 600 s) but from the temperature profiles it can be noted that the junction temperature in the no-foam case (around 70 °C), exceeds that of melting point. With foam, however, the junction temperature is lower than that of melting point (around 50 °C). Besides, the thermocouples located 5 mm over the heated walls show different behaviours. When the foam is used to enhance the heat transfer, the temperature is very close to that of the junction, whereas with no foams the reading is about 30 K lower than that of the junction.
- After the first 20 min (i.e. 1200 s), as it can be seen in the two frames, the melting process is started in the case of no-foam paraffin wax, whereas with the 5 PPI foam no liquid region can be detected. According to the temperature profiles, the junction temperature in the case without foam is quickly approaching 90 °C (black dotted line) whereas when the foam is used, it is at around 61 °C. The first thermocouples ( $H = 5$  mm) measure 67 °C and 58 °C, in the case without and with foam, respectively.
- The results after 30 min (i.e. 1800 s) clearly highlight the interesting heat transfer capabilities of the foam when used as conductive structure to improve the phase change process. In fact, the two systems show almost the same level of liquid paraffin, around 35% but the system that uses the foam has a junction temperature (around 69 °C) lower than the temperature measured by the thermocouple inserted in the liquid paraffin of no-foam sample (around 74 °C). The temperature of the liquid paraffin in the case with foam remains close to the junction one being around 66 °C.
- With foam, the PCM fusion process is complete after around 40 min with the junction temperature lower than 80 °C. At this point in time, only 62.5% of the paraffin is melted and its liquid temperature is around 22 K superheated while the junction temperature is close to 100 °C.

The complete sequence can be watched by playing the attached video 1, which compares the two cases with and without foam. Analysis of the images, makes clear that there are strong convective motions in the superheated liquid paraffin wax without foam; a trend which cannot be observed when the foam is used.

This also confirms results reported by Tian and Zhao [16] that due to a large flow resistance the foam suppressed the natural convection flow. Higher PPI foams lead to even higher flow resistances. As such, if a low PPI sample, 5 PPI, suppresses the buoyancy-induced flow then obviously higher PPI values are expected to do the same. Finally, one observes that using the foam as heat transfer medium, the melting process is faster but the maximum junction temperature is around 20 K lower than that measured without foam.

Fig. 8 compares the melting process of the same 5203 paraffin wax embedded in the 5 PPI copper foam at two different heat fluxes: 12.5 (i.e. 20 W) and 18.75  $\text{kW m}^{-2}$  (i.e. 30 W). Four time steps are considered: 10, 15, 20, and 30 min; the dotted lines refer to 20 W whereas the solid lines to 30 W.

- As expected the temperatures measured at 30 W are higher than those measured at 20 W. After the first 10 min, no

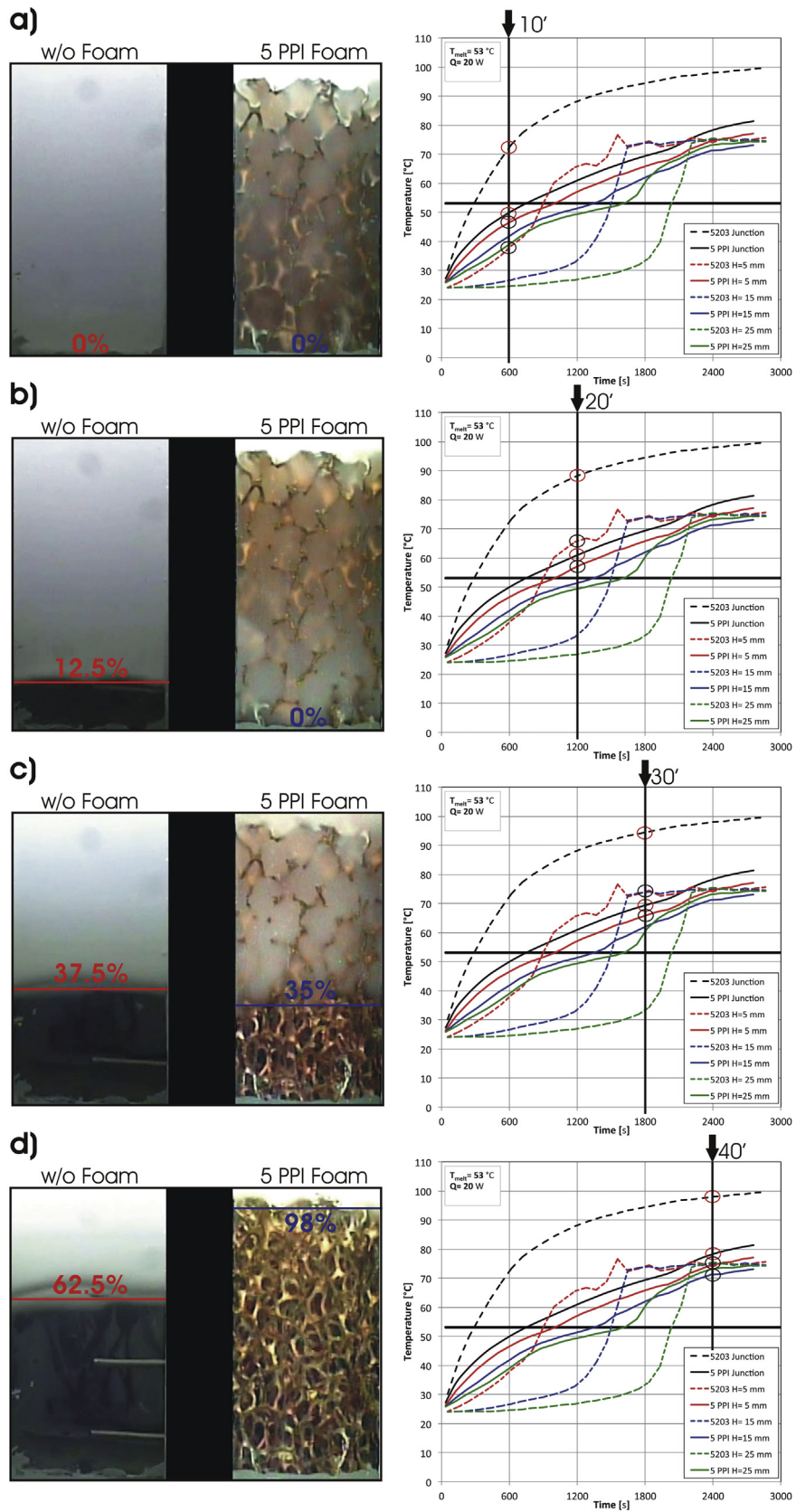


Fig. 7. Phase change process with and without 5 PPI copper foam of Sasolwax 5203 at 20 W.

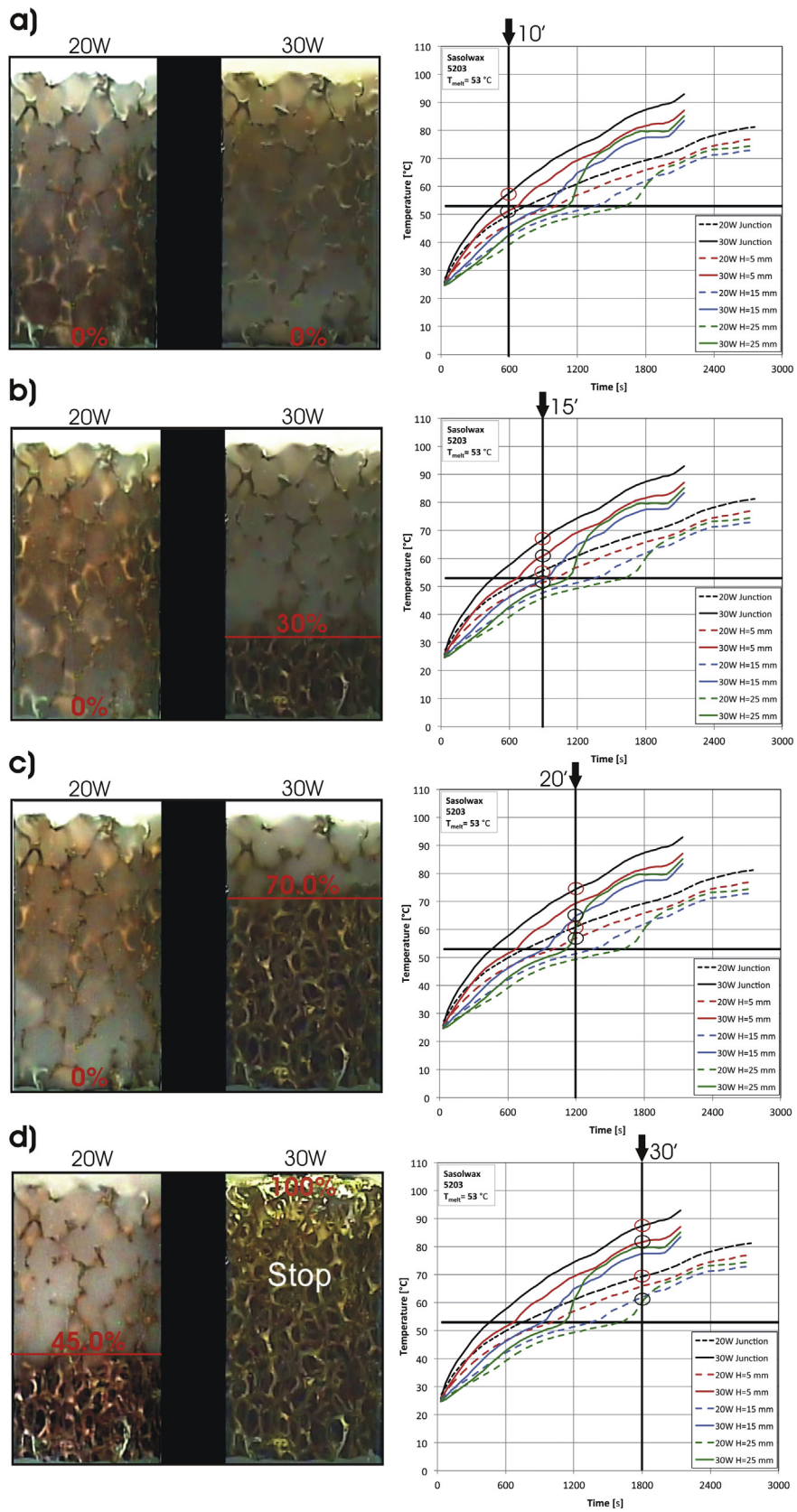


Fig. 8. Comparison of the phase change process of Sasolwax 5203 embedded in 5 PPI copper foam at 20 W and 30 W.

evidence of fusion can be noticed. As indicated in the charts, the junction temperature in the two cases is almost around the melting point: 57 °C at 30 W and 50 °C at 20 W.

- Five minutes later, at 15', around 30% of the paraffin wax is already melted at 30 W while at lower heat flow rate it is solid.
- This situation remains the same after 20': no evidence of melting process can be noticed at 20 W while at 30 W around the 70% of the paraffin wax is liquefied. At that moment the junction temperature has reached 75 °C at 30 W while it is around 60 °C at 20 W.
- After 30', the melting process at 30 W is concluded while just around 45% of the paraffin wax is melted at 20 W. The maximum junction temperature at 30 W is slightly lower than 90 °C and it is around 20 K higher than that measured at 20 W. Considering the other thermocouples, it can be stated that the temperature profiles measured at 20 and 30 W are similar. More details can be found in the video 2, downloadable as supplementary data, which compares the phase change process of the analysed cases.

Supplementary video related to this article can be found at <http://dx.doi.org/10.1016/j.ijthermalsci.2014.11.023>.

Fig. 9 reports two examples of implementation of different copper foams: in particular, Fig. 9a shows the melting process of the 5203 paraffin wax embedded in a 20 PPI foam at 20 W, whereas Fig. 9b plots the temperature profiles recorded at 30 W during the fusion of the same paraffin wax embedded in a 40 PPI copper foam.

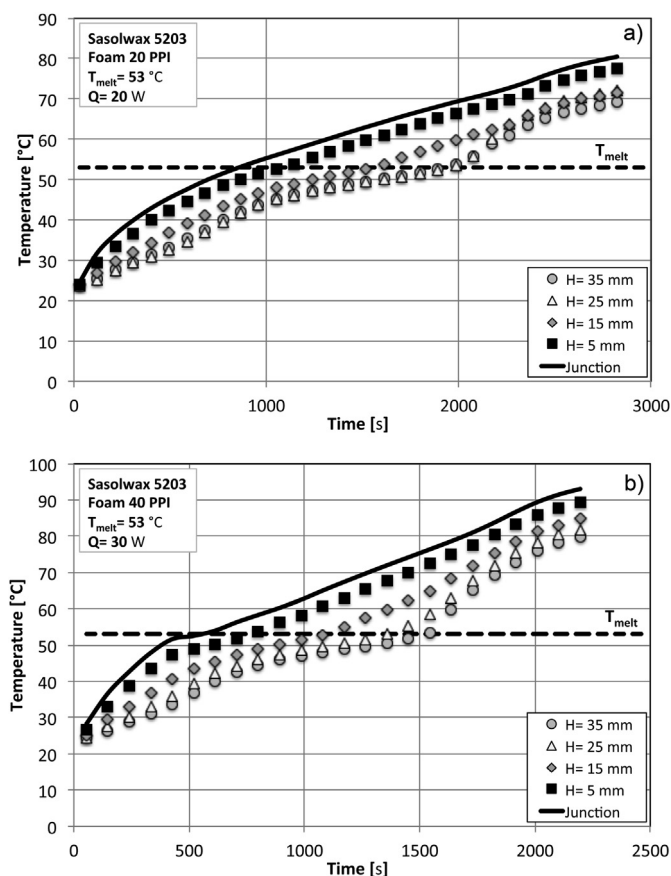


Fig. 9. Temperature profiles: (a) 10 PPI copper foam embedded with paraffin wax 5203 at  $Q = 20\text{ W}$ ; (b) 40 PPI copper foam embedded with paraffin wax 5203 at  $Q = 30\text{ W}$ .

Even though the maximum temperatures achieved must be different because the imposed heat flux is higher in the case of 40 PPI foam as compared to the case of 20 PPI foam, the temperature profiles are similar. As already mentioned in the case of 5 PPI foam, the temperature difference between the values measured by the junction and the top thermocouples are very low during all the melting process meaning that the foam acts as a heat spreader transferring the heat throughout the paraffin wax and not just through the solid–liquid interface unlike the no-foam case. Fig. 10 reports a photo of the 5 PPI copper foam and a particular of the porous structure that was reconstructed using micro-tomography scans, as proposed in Diani et al. [25]. The heat that comes from the copper plate, to which the copper foams are brazed, can be transferred through the porous structures through several different paths; some of those are highlighted using different coloured dotted lines. The heat flows through the interconnected fibres by virtue of their high thermal conductivity (around  $390\text{ W m}^{-1}\text{ K}^{-1}$ ), which is three orders of magnitude greater than that of the paraffin wax. These considerations explain the heat transfer performance of the foam–paraffin systems. In fact, as already described, the melting process starts earlier in the case of the no-foam paraffin, but when it starts in the foam–paraffin samples, it becomes faster and the temperatures are much lower because the heat is effectively transferred throughout the solid being not confined in the liquefied paraffin as in the case without foam.

As described before, it has to be underlined that the benefits obtained using the copper foams as heat transfer medium would be completely lost if the foams were not brazed over the surface because a high contact resistance with an apparent low thermal conductivity similar to that of the paraffin would be introduced; see Refs. [21–23].

There is another interesting advantage in the use of the metallic foams in PCM applications. The porous structure enhances the paraffin solidification process. In particular, when an asymmetric heat flux is imposed, the melting process starts from the heated surface and the liquid–solid interface moves forward through the solid. When the heat load is removed, the solidification of paraffin starts from the unheated (colder) side walls. This asymmetric solidification process associated with the decrease of the volume is linked to the liquid–solid phase change and implies that a void volume can be generated in the centre of the module, limiting its applicability in cyclic systems. When a porous structure is used as heat transfer medium, this drawback is mitigated and the solidification process proceeds uniformly. After a phase change cycle, the foam–paraffin system returns to the same state ensuring that a reliable and effective passive cooling can be repeated.

Fig. 11 compares all the tested configurations: the no-foam paraffin and the three different foam–paraffin samples, plotting

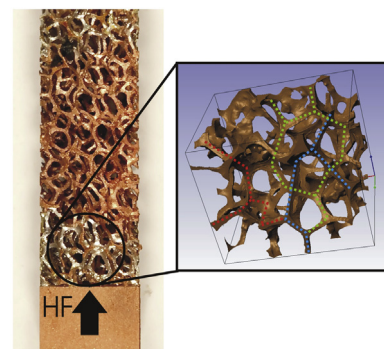


Fig. 10. Photo of a 5 PPI copper foam with a particular reconstructed via micro-tomography scans.

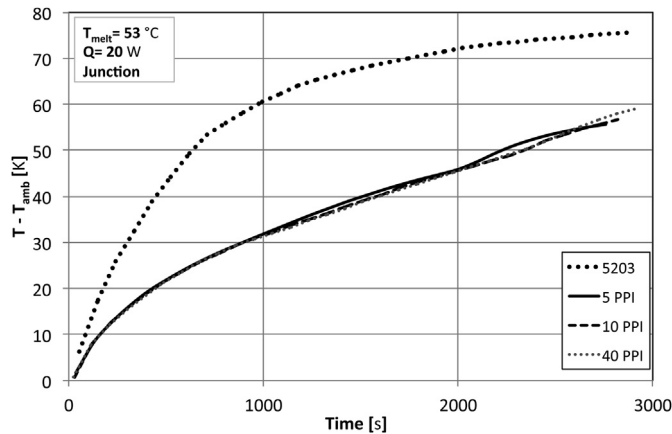


Fig. 11. Comparison between the investigated configuration with and without foam at constant imposed heat flow rate of 20 W.

the junction to ambient temperature difference measured at  $HF = 12.5 \text{ kW m}^{-2}$  as a function of time. Furthermore, Table 3 compares the values of the junction to ambient temperature difference of the tested configurations with and without foam measured at different time steps at the three imposed heat loads. From the combined analysis of the diagram, and of the values listed in Table 3, one notes that all the paraffin-foam systems exhibit almost the same behaviour and there is not any optimal foam configuration. This can be explained considering how the foam structure may affect the heat distribution through the PCM, see Fig. 10. This approach was also used by Tamayol and Hooman [26] in modelling the foam structure as a matrix of interconnected solid ligaments that allows conduction heat transfer and interfacial convection to the passing fluid, including a thermal contact resistance between the fibres and the heated wall. In the present case, the heat is spread by the high conductive fibres of the foam, heating up the paraffin wax, which, unfortunately, has a very low thermal conductivity that limits the overall heat transfer performance. This might explain why heat transfer performance seems to be independent on the pore density: the interconnected fibres conduct effectively the heat but then heat transfer is finally limited by the low thermal conductivity of the paraffin wax. This is in line with Thapa et al.'s [20] suggestion of using copper foam to enhance the apparent thermal conductivity of the PCM assembly but they also

Table 3  
Comparison between the investigated configurations with and without foam at the three investigated heat loads.

Q [W]	Time [s]	$T_j - T_{amb}$ [K]			
		5203	5 PPI	10 PPI	40 PPI
10	0	0	0	0	0
	600	24.6	13.3	13.0	12.4
	1200	36.4	20.3	19.1	19.0
	2400	46.3	28.9	28.6	27.3
	3600	50.3	34.4	33.4	32.3
	6000	54.3	45.8	45.5	45.4
20	0	0	0	0	0
	600	48.3	24.2	24.1	24.1
	1200	64.3	35.2	34.5	34.3
	1800	70.5	43.1	43.1	42.9
	2400	73.9	52.6	51.2	51.3
	2800	75.4	55.9	56.5	57.8
30	0	0	0	0	0
	300	44.6	21.5	22.8	21.7
	600	67.6	33.2	33.8	29.5
	1200	86.7	49.8	50.4	43.8
	1800	94.2	62.8	63.8	58.8
	2100	96.5	67.1	68.7	67.1

highlighted the phenomenon of the diminishing returns as conductivity exceeded  $4\text{--}6 \text{ W m}^{-1} \text{ K}^{-1}$ . In particular, according to [20], the performance tends to flatten and the achievable improvement diminishes over a certain value of the apparent thermal conductivity. This phenomenon might explain why there is not any remarkable effect of the pore density on the heat transfer performance of the present samples.

## 6. Conclusions

This paper investigates the solid–liquid phase change process of three natural paraffin waxes with similar melting temperatures:  $53 \text{ }^\circ\text{C}$ ,  $57 \text{ }^\circ\text{C}$ , and  $59 \text{ }^\circ\text{C}$ , at three imposed heat fluxes:  $6.25$ ,  $12.5$ , and  $18.75 \text{ kW m}^{-2}$  corresponding to  $10 \text{ W}$ ,  $20 \text{ W}$ , and  $30 \text{ W}$ , respectively.

The paraffin waxes performed similarly and the maximum junction temperatures reached around  $80 \text{ }^\circ\text{C}$ ,  $100 \text{ }^\circ\text{C}$ , and  $120 \text{ }^\circ\text{C}$  at  $6.25$ ,  $12.5$ , and  $18.75 \text{ kW m}^{-2}$ , respectively; accordingly, the melting time decreases as the heat flux increases.

One of the main drawbacks related to the application of the paraffin wax is linked to its low thermal conductivity, which obstacles the heat transfer. The melted liquid becomes superheated (for example around  $15 \text{ K}$  at  $6.25 \text{ kW m}^{-2}$ ) and the junction temperature reaches very high values. Another relevant problem is linked to the non-uniform solidification in asymmetric heating configuration, which might imply some reliability issues in intermittent hot devices, typical of these applications.

This work demonstrates the interesting heat transfer enhancement achievable with the use of copper foams as heat transfer medium in PCM systems. One paraffin wax, 5203, was embedded in three different foam matrixes with 5, 10, and 40 PPI with constant porosity of 0.94 and then tested by imposing the same heat fluxes as the case without foam. There is not any noticeable difference between the three copper foams investigated; anyway, the reached maximum junction temperatures were much lower as compared to the case without foam.

The foam structure was found to enhance the heat transfer properties of the paraffin wax acting as a heat spreader directly embedded in the PCM; this feature allows for a uniform distribution of the temperature inside the PCM, the onset phase change process is delayed but it ends earlier meaning that the heat is distributed throughout the PCM and not just at the liquid–solid interface. These results are also confirmed by the video recorded. Furthermore, the use of the copper foam structure permits to eliminate the serious solidification issues associated to the asymmetric heating, which limit the use of the paraffin waxes in passive cyclic electronic cooling systems.

This work highlights the interesting heat transfer capabilities of the foam-paraffin wax systems as passive heat transfer solution for electronic thermal management. Additional work is surely needed to develop and characterize some different prototypes to be tested in real operating conditions.

## Acknowledgement

The support of SasolWax GmbH is gratefully acknowledged.

## References

- [1] B. Zalba, J.M. Marín, L.F. Cabeza, H. Mehling, Review on thermal energy storage with phase change: materials, heat transfer analysis and applications, *Appl. Therm. Eng.* 23 (2003) 251–283.
- [2] A. Sharma, V.V. Tyagi, C.R. Chen, D. Buddhi, Review on thermal energy storage with phase change materials and applications, *Renew. Sustain. Energy Rev.* 13 (2009) 318–345.
- [3] F. Agyenim, N. Hewitt, P. Eames, M. Smyth, A review of materials, heat transfer and phase change problem formulation for latent heat thermal energy storage systems (LHTES), *Renew. Sustain. Energy Rev.* 14 (2010) 615–628.

- [4] M. Xiao, B. Feng, K. Gong, Thermal performance of a high conductive shape-stabilized thermal storage material, *Sol. Energy Mater. Sol. Cells* 69 (2001) 293–296.
- [5] S. Jegadheeswaran, S.D. Pohekar, Performance enhancement in latent heat thermal storage system: a review, *Renew. Sustain. Energy Rev.* 13 (2009) 2225–2244.
- [6] L. Fan, J.M. Khodadadi, Thermal conductivity enhancement of phase change materials for thermal energy storage: a review, *Renew. Sustain. Energy Rev.* 15 (2011) 24–46.
- [7] R. Baby, C. Balaji, Experimental investigations on phase change material based finned heat sinks for electronic equipment cooling, *Int. J. Heat Mass Transfer* 55 (2012) 1642–1649.
- [8] R. Baby, C. Balaji, Thermal optimization of PCM based pin fin heat sinks: an experimental study, *Appl. Therm. Eng.* 54 (2013) 65–77.
- [9] R. Baby, C. Balaji, Thermal performance of a PCM heat sink under different heat loads: an experimental study, *Int. J. Therm. Sci.* 79 (2014) 240–249.
- [10] L.-W. Fan, Y.-Q. Xiao, Y. Zeng, X. Fang, X. Wang, X. Xu, Z.-T. Yu, R.-H. Hong, Y.-C. Hu, K.-F. Cen, Effects of melting temperature and the presence of internal fins on the performance of a phase change material (PCM)-based heat sink, *Int. J. Therm. Sci.* 70 (2013) 114–126.
- [11] S. Mahmoud, A. Tang, C. Toh, R. AL-Dadah, S.L. Soo, Experimental investigation of inserts configurations and PCM type on the thermal performance of PCM based heat sinks, *Appl. Energy* 112 (2013) 1349–1356.
- [12] Y. Kozak, B. Abramzon, G. Ziskind, Experimental and numerical investigation of a hybrid PCM-air heat sink, *Appl. Therm. Eng.* 59 (2013) 142–152.
- [13] S.-T. Hong, D.R. Herling, Open-cell aluminum foams filled with phase change materials as compact heat sinks, *Scr. Mater.* 55 (2006) 887–890.
- [14] O. Mesalhy, K. Lafdi, A. Elgafy, Carbon foam matrices saturated with PCM for thermal protection purposes, *Carbon* 44 (2006) 2080–2088.
- [15] C.Y. Zhao, W. Lu, Y. Tian, Heat transfer enhancement for thermal energy storage using metal foams embedded within phase change materials (PCMs), *Sol. Energy* 84 (2010) 1402–1412.
- [16] Y. Tian, C.Y. Zhao, A numerical investigation of heat transfer in phase change materials (PCMs) embedded in porous metals, *Energy* 36 (2011) 5539–5546.
- [17] D. Zhoua, C.Y. Zhao, Experimental investigations on heat transfer in phase change materials (PCMs) embedded in porous materials, *Appl. Therm. Eng.* 31 (2011) 970–977.
- [18] H.T. Cui, Experimental investigation on the heat charging process by paraffin filled with high porosity copper foam, *Appl. Therm. Eng.* 39 (2012) 26–28.
- [19] R. Baby, C. Balaji, Experimental investigations on thermal performance enhancement and effect of orientation on porous matrix filled PCM based heat sink, *Int. Commun. Heat Mass Transfer* 46 (2013) 27–30.
- [20] S. Thapa, S. Chukwu, A. Khaliq, L. Weiss, Fabrication and analysis of small-scale thermal energy storage with conductivity enhancement, *Energy Convers. Manag.* 79 (2014) 161–170.
- [21] T. Fiedler, N. White, M. Dahari, K. Hooman, On the electrical and thermal contact resistance of metal foam, *Int. J. Heat Mass Transfer* 72 (2014) 565–571.
- [22] M. Odabae, S. Mancin, K. Hooman, Metal foam heat exchangers for thermal management of fuel cell systems – an experimental study, *Exp. Therm. Fluid Sci.* 51 (2013) 214–219.
- [23] P. De Jaeger, C. T'Joan, H. Huisseune, B. Ameel, S. De Schampheleire, M. De Paepe, Assessing the influence of four cutting methods on the thermal contact resistance of open-cell aluminum foam, *Int. J. Heat Mass Transfer* 55 (2012) 6142–6151.
- [24] S. Mancin, C. Zilio, A. Diani, L. Rossetto, Air forced convection through metal foams: experimental results and modeling, *Int. J. Heat Mass Transfer* 62 (2013) 112–123.
- [25] A. Diani, K. Bodla, L. Rossetto, S.V. Garimella, Numerical analysis of air flow through metal foams, *Energy Procedia* 45 (2014) 645–652.
- [26] A. Tamayol, K. Hooman, Thermal assessment of forced convection through metal foam heat exchangers, *J. Heat Transfer* 133 (2011) 111801–1–111801-7.